

# Circular Dichroism of Heterochromophoric and Partially Regenerated Purple Membrane: Search for Exciton Coupling

ELENA KARNAUKHOVA,<sup>1</sup> CHRYSOULA VASILEIOU,<sup>2</sup> ANDY WANG,<sup>3</sup> NINA BEROVA,<sup>3</sup>  
 KOJI NAKANISHI,<sup>3\*</sup> AND BABAK BORHAN<sup>2\*</sup>

<sup>1</sup>Center for Biologics Evaluation and Research, Food and Drug Administration, Bethesda, Maryland 20892

<sup>2</sup>Department of Chemistry, Michigan State University, East Lansing, Michigan 48824

<sup>3</sup>Department of Chemistry, Columbia University, New York, New York 10027

**ABSTRACT** In order to determine the origin of the bisignate CD spectra of native purple membrane, heterochromophoric analogues containing bacteriorhodopsin regenerated with native *all-trans*-retinal and retinal analogues were investigated. The data collected for the purple membrane samples containing two different chromophores suggest the additive character of the CD spectra. This conclusion was supported by a series of spectra using 5,6-dihydroretinal and 3-dehydroretinal and by using 33% regenerated PM in buffer and in presence of osmolytes. Our results support the idea of conformational heterogeneity of the chromophores in the bR in the trimer, suggesting that the three bR subunits in the trimer are not conformationally equal, and therefore, the bisignate CD spectrum of bR in the purple membrane occurs rather due to a superposition of the CD spectra from variously distorted bR subunits in the trimer than interchromophoric exciton-coupling interactions. © 2005 Wiley-Liss, Inc. *Chirality* 18:72–83, 2006.

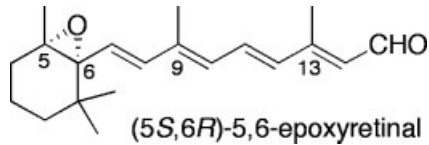
**KEY WORDS:** purple membrane; bacteriorhodopsin; partial regeneration; heterochromophoric; circular dichroism; exciton-coupled circular dichroism

Bacteriorhodopsin (bR),<sup>1</sup> the single integral protein of the purple membrane (PM) of *Halobacterium halobium*, functions as a light-activated proton translocase and is one of the best-studied membrane proteins.<sup>2</sup> Similar to rhodopsin, it consists of seven transmembrane helices and short interhelical loops bearing extramembrane N and C termini. The native chromophore, *all-trans*-retinal, is bound to the ε-amino group of Lys-216 via a protonated Schiff base (PSB).<sup>3–5</sup> Bacteriorhodopsin molecules in the PM are arranged in clusters of three (trimers) which form two-dimensional hexagonal crystals with  $P_3$  symmetry.<sup>6–10</sup>

Figure 1a depicts the crystallized form of the trimeric form and the monomeric unit of bR trimer.<sup>11–13</sup> The chromophore lies in the intramembrane cavity formed by the seven helices with its conjugated polyene chain nearly perpendicular to the membrane.<sup>11–14</sup> The chromophoric plane (defined as the conjugated polyene excluding the ionone ring) is tilted up slightly (20.5° with respect to the lipid bilayer), which disposes the β-ionone ring toward the extracellular side of the membrane, close to helices D and E (Fig. 1b). The distance between the chromophores within the same trimer is ~26 Å.<sup>11,13</sup> Neutron diffraction studies have determined the intertrimeric chromophore–chromophore distance to be 38 Å.<sup>15</sup>

The CD spectra of bR and synthetic analogues have been used widely to investigate the arrangements of bR in the membrane,<sup>16</sup> the protein conformational changes,<sup>17,18</sup> and the photocycle intermediates.<sup>19–22</sup> The CD of native

bR and many artificial analogues show bisignate curves of opposite sign centered at the absorption maxima of the chromophores. As shown in Figure 1c, in the case of the natural substrate, *all-trans*-retinal, the CD spectrum consists of a negative first Cotton effect (CE) at 593 nm, followed by a positive second CE at 531 nm. The cross-point is located at 560 nm, very close to the corresponding  $\lambda_{\text{max}}$  (557 nm). However, this is not always the case: (i) bR incorporating (5S,6R)-5,6-epoxyretinal yields a hexagonal



lattice (X-ray diffraction) with an absorption at 485 nm and exhibits a bisignate CD, 460 nm (+)/520 nm (–); in contrast, bR with the enantiomeric (5R,6S)-chromophore is paracrystalline as in the apo-membrane, absorbs at 445 nm,

Contract grant sponsors: NIH, NSF; Contract grant numbers: GM 36564, Career Grant CHE-0094131

\*Correspondence to: Babak Borhan, Michigan State University, Department of Chemistry, East Lansing, MI 48824. E-mail: babak@chemistry.msu.edu

Received for publication 7 July 2005; Accepted 27 September 2005

DOI: 10.1002/chir.20222

Published online in Wiley InterScience (www.interscience.wiley.com).

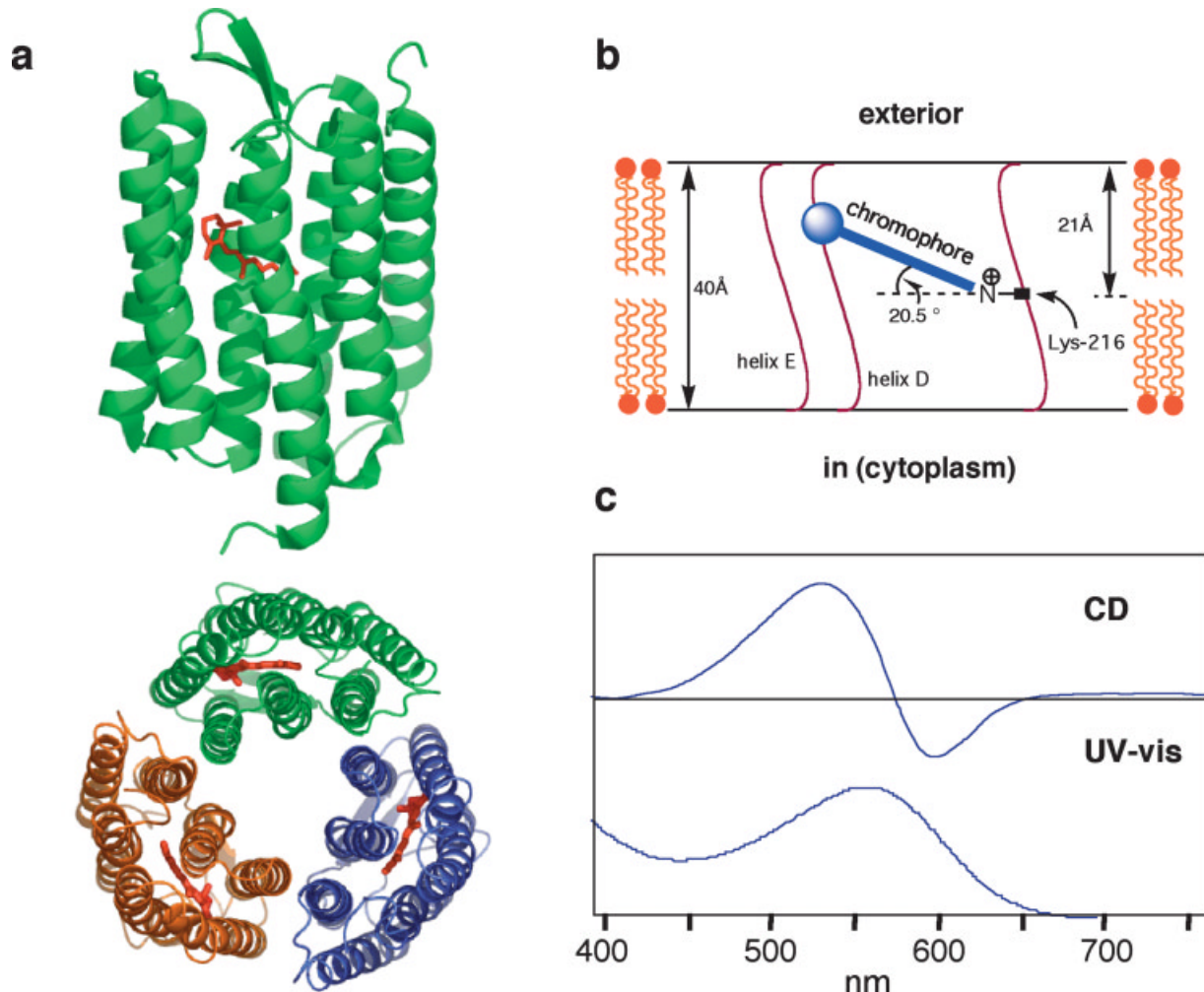


**Fig. 1.** (a) Crystal structure of bR in the purple membrane. (b) Schematic representation of the cross-section of bR. Retinal is linked to Lys 216 located around the midpoint of the membrane. (c) UV-vis and CD spectra of native bR in 20 mM sodium phosphate buffer, pH 7.0.

and exhibits a positive CD at 435 nm.<sup>23</sup> (ii) Reduced Schiff base of bR (treated with sodium borohydride), which retains the hexagonal structure, shows only a monophasic positive CD band.<sup>24,25</sup> These data clearly demonstrate the complexity of the nature of the CD spectra.

The biphasic CD spectrum has been interpreted as a superposition of an intrinsic positive CE arising from the protein environment and a bisignate CD due to exciton coupling (EC) within the bR trimer.<sup>19,26–30</sup> However, a number of other explanations for the origin of the biphasic CD have been proposed that dismiss excitonic coupling.<sup>24,31–33</sup> One suggestion is that the bisignate CD is due to the superposition of two close-lying long-wavelength transitions with opposite signs.<sup>26,32,34</sup> Alternatively, it has been suggested that the biphasic CD is the result of the superposition of multiple intrinsic CD bands arising from different tertiary structures in the membrane.<sup>30</sup> Although the CD of bR and analogues have been extensively studied and reviewed,<sup>30,32,35,36</sup> the origin of the biphasic CD spectra remains unclear.

To further investigate the origin of the biphasic CD spectrum of bR, two different approaches were utilized. *Chirality DOI: 10.1002/chir*

In addition to native *all-trans*-retinal **A**, we have incorporated three analogues with different absorption maxima upon binding with apo-membrane, merocyanine aldehyde **B** (646 nm), 3-dehydroretinal **C** (594 nm), and *cis*-5,6-dihydroretinal **D** (467 nm), into the apo-membrane in a stepwise manner and in various ratios in order to form homochromophoric and heterochromophoric pigments in the trimeric form of bR (Fig. 2). The potential interaction of the chromophores within the trimers were investigated in accordance with rules of ECCD for coupling of degenerate and nondegenerate chromophores.<sup>37,38</sup> As a second approach, the spectra of partially regenerated purple membrane (33% regeneration, only one chromophore present per bR trimer) were recorded in the presence of osmotically active agents (sucrose, glycerol) in an attempt to probe the effect of conformational flexibility of the membrane/protein complex on the shape of the CD spectra. In the presence of a single chromophore, exciton coupling is excluded, and thus, the shape of the CD spectrum depends solely on the induced chirality of the bound chromophore. The CD data obtained for the various fully and partially reconstituted pigments have led us to

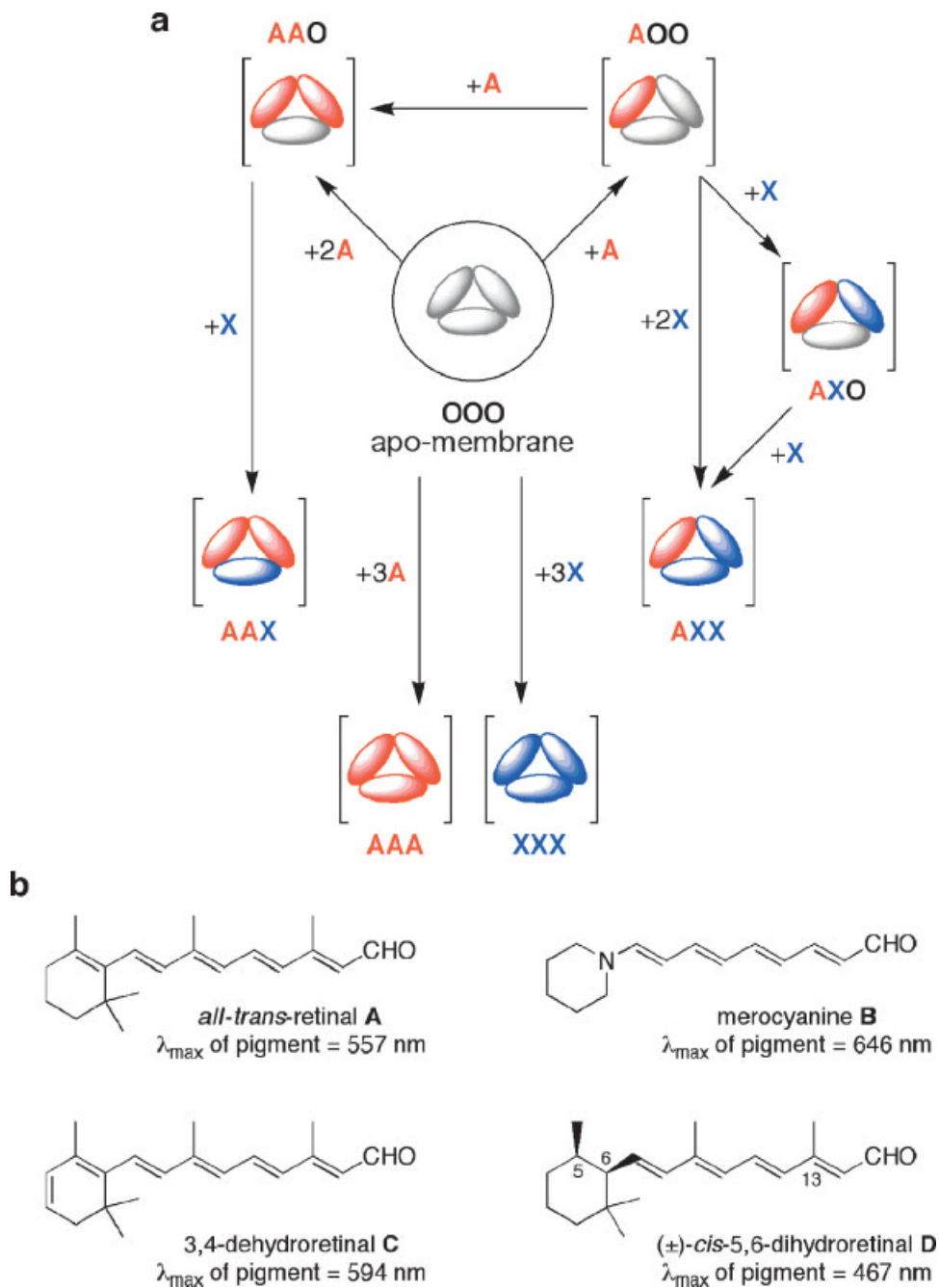


**Fig. 2.** (a) Schematic representation of the stepwise reconstitution of apo-membrane (OOO) to either fully (AAA) or partially (AOO, AAO) reconstituted PM. X represents the retinal analogues used for homochromophoric and heterochromophoric reconstitution. (b) Native substrate of bR *all-trans*-retinal (A) and the analogues used (**B–D**).  $\lambda_{\text{max}}$  of the pigment refers to the absorption of the fully occupied membrane with each chromophore.

conclude that the apparent bisignate CD spectra result from the summation of CE of opposite signs rather than exciton coupling between the pigments of the bR trimer.

## MATERIALS AND METHODS

All experiments described herein have been carried out using large membrane patches (PM or apo-membrane) in order to preserve the membrane structure and the trimeric

form. The membranes used in this study were all dark-adapted. Control measurements of light-adapted PM (containing homogeneous all-trans chromophore) showed similar results. The PM was isolated by the conventional procedure<sup>1</sup> with an  $A_{278}/A_{560}$  ratio of 1.76 and bleached in 1 M NH<sub>2</sub>OH at pH 7.6 as previously described.<sup>24</sup> The membrane protein samples were stored in the presence of sodium azide (0.05%) at -70°C in order to prevent proteolytic digestion, and the identity of the initial PM prep-

arations was checked before use by UV-vis ( $A_{278}/A_{560}$  ratio) and CD ( $A_{530}/A_{598}$  ratio). UV-vis spectra were recorded on PerkinElmer 320 spectrophotometer using 1-cm path length quartz cells. CD spectra were recorded on a JASCO Model 720 spectropolarimeter immediately after absorption measurement using optical cells of 1-cm path length at room temperature (20°C).

### Apo-Membrane

The apo-membrane was generated as described previously through bleaching of the purple membrane.<sup>24</sup> Before regeneration, the apo-membrane was subjected to additional purification using a sucrose gradient (25–45%), and the fraction at ~40% density was collected, washed three times with deionized water, and finally resuspended in 20 mM sodium phosphate buffer, pH 7.0. Preparation of the apoprotein was performed with and without removal of retinal oxime using bovine serum albumin.<sup>39</sup>

### Chromophores

The merocyanine dye was synthesized as described earlier,<sup>40</sup> stored as the Schiff base, and hydrolyzed to aldehyde **B** immediately before binding with the apo-membrane. 3-Dehydroretinal **C** was obtained from *all-trans*-retinal in two steps as previously described.<sup>41</sup> ( $\pm$ )-*cis*-5,6-Dihydroretinal **D** was also prepared according to reported protocols.<sup>42,43</sup>

### Preparation of Pigments (Fig. 2)

For binding experiments, the calculated amount of *all-trans*-retinal or retinal analogue in ethanolic solution (final ethanol concentration was kept at <1% by volume) was added to the apo-protein in phosphate buffer (identical concentration of apo-membrane stock solution was used) and the mixture was incubated for 8 h under stirring in the dark at room temperature (20°C) and monitored by UV-vis and CD. PM was regenerated using 1.5 equiv of retinal (excess retinal is required for complete binding<sup>44</sup>). Homochromophoric pigments **BBB**, **CCC**, and **DDD** were obtained in a similar manner using retinal analogues **B**, **C**, and **D**, respectively. Due to instability of the merocyanine aldehyde **B**, an additional amount of freshly prepared chromophore was added 4 h later to ensure complete reconstitution of the apoprotein with the chromophore to yield a fully saturated system. The  $\epsilon$  of mc-bR **BBB** was estimated to be 69,000 M<sup>-1</sup> cm<sup>-1</sup> by assuming that the binding yield is similar to that of PM regeneration at equal apoprotein concentration. The absorbance at the  $\lambda_{\text{max}}$  of the fully regenerated dark-adapted pigment was used to estimate the equivalence or percentage of pigment regeneration. The  $\lambda_{\text{max}}$  and  $\epsilon$  of the dark-regenerated pigments are as follows: bR (**AAA**) 557 nm, 52,000 M<sup>-1</sup> cm<sup>-1</sup>; mc-bR (**BBB**) 646 nm,  $\epsilon$  = 69,000 M<sup>-1</sup> cm<sup>-1</sup>; 3-dehydro-bR (**CCC**, “Blue Membrane”),<sup>45</sup> 594 nm,  $\epsilon$  = 47,000 M<sup>-1</sup> cm<sup>-1</sup>; and *cis*-5,6-dihydro-bR (**DDD**),<sup>43,46</sup> 467 nm,  $\epsilon$  = 40,000 M<sup>-1</sup> cm<sup>-1</sup>.

### Partially Regenerated Purple Membrane AOO and AAO

The 33% regenerated PM (**AOO**) was used as starting material for heterochromophoric samples **AXO** and **AXX**. Chirality DOI: 10.1002/chir

Regeneration of the known amount of apo-membrane to 33% was achieved using 0.33 equiv of *all-trans*-retinal. Binding to the apo-membrane was evaluated by CD spectroscopy. The single positive CD band observed for 33% regenerated PM indicated the presence of predominantly only one chromophore per bR trimer resulting from the even distribution of the chromophores within the membrane. The 66% regenerated PM (**AAO**) was obtained in a similar manner and was also monitored with UV-vis and CD spectroscopy (note: the sucrose studies described below utilized 33%, 50%, and fully regenerated PM). The percentage of regeneration was confirmed by UV-vis spectra via correlation with the fully regenerated apo-membrane as a reference.

### Preparation of Heterochromophoric Membrane Samples

**ABO** (bR/mc-bR, 1:1:0) was obtained by further reconstitution of **AOO** (33% regenerated PM) with 0.33 equiv of merocyanine analogue **B**. **AAB** (mc-bR/bR, 2:1) was prepared by addition of merocyanine aldehyde **B** to 66% regenerated PM (**AAO**). **ABB** (mc-br/bR, 1:2) was prepared by addition of merocyanine aldehyde **B** to **ABO**. Other **AXO** and **AXX** heterochromophoric samples were obtained similarly using 3-dehydroretinal (**C**) or 5,6-dihydroretinal (**D**).

### Change of the Pigment Media by a Precipitation/Resuspension Procedure

In order to monitor the solvent-induced reversible conformational changes for partially regenerated purple membrane in various solutions, 2.5 ml of a suspension of 33% regenerated PM (0.85 OD) in phosphate buffer (pH 7.0) was concentrated to 0.9 ml using Amicon filters (10,000 MW cutoff) and sonicated for 10 s, and the UV-vis and CD spectra were recorded. The sample was then spun down at 27,000 rpm, the pellet was resuspended in 50% sucrose in phosphate buffer (0.9 ml), sonicated (10 s), and used for the second UV-vis and CD measurements. The same 33% regenerated sample was subsequently resuspended in the 35% sucrose (or glycerol) solution, and the corresponding UV-vis and CD spectra were recorded. For each preparation, corresponding spectra were also recorded in phosphate buffer as well in order to assure the reversible character of the observed conformational changes.

## RESULTS AND DISCUSSION

The experiments detailed below were designed to investigate the principal cause that leads to the bisignate CD spectrum observed for bR in the PM. According to the published crystal structure of the bR, the distances between the retinal molecules within the trimeric form can allow for exciton coupling.<sup>37,38</sup> Because the objective is to ascertain whether the bisignate CD spectrum observed is due to excitonic coupling between the chromophores in the bR trimer, proper understanding of the corresponding arguments is critical.

Exciton-coupled circular dichroism (ECCD) spectra arise from the through-space interaction of the electric

transition dipole moments of two or more independently conjugated chromophores that are chirally disposed.<sup>37,38</sup> The basic principles of the ECCD method that are directly associated with the present discussion are as follows:

- (i) The  $A$  value, i.e., the difference in  $\Delta\epsilon$  values of the two extrema of an exciton split curve is inversely proportional to  $R^2$ , the square of interchromophoric distances.
- (ii) The  $A$  value is proportional to the square of the molecular extinction coefficient of the coupled chromophores ( $\epsilon^2$ ).<sup>16</sup> Chromophores with strong absorption, such as porphyrins (Soret band  $\lambda_{\text{max}}$  at 415 nm,  $\epsilon = 350,000 \text{ M}^{-1} \text{ cm}^{-1}$ ), couple at distances of  $>50 \text{ \AA}$ .<sup>47-49</sup>
- (iii) In vicinal systems, the  $A$  value is maximal at a chromophoric projection angle of ca. 70°.
- (iv) In bichromophoric systems, exciton coupling occurs even when the absorption maxima of the two chromophores differ by 9,000 cm<sup>-1</sup>, as has been shown experimentally and theoretically for the *p*-bromobenzoate ( $\lambda_{\text{max}}$  244 nm,  $\epsilon = 19,500 \text{ M}^{-1} \text{ cm}^{-1}$ )/*p*-dimethylaminobenzoate system ( $\lambda_{\text{max}}$  307 nm,  $\epsilon = 28,500 \text{ M}^{-1} \text{ cm}^{-1}$ ) coupling, where the difference is ca. 8,500 cm<sup>-1</sup>.
- (v) In systems containing two different chromophores, two opposite Cotton effects appear, slightly red- and blue-shifted from the respective maxima of the non-interacting chromophores.
- (vi) The principle of pairwise additivity holds in systems comprising of three or more chromophores. For example, in 130 hexapyranoses substituted with *p*-bromobenzoate and *p*-methoxycinnamate, the observed CDs are in excellent agreement with the pairwise summation curves.<sup>50</sup> This is also supported by theoretical calculations.<sup>51</sup>

In the work described herein, we plan to exploit the fact that nondegenerate chromophores, with close  $\lambda_{\text{max}}$ , can efficiently couple through space to yield ECCD spectra. In particular, by using homo- and heterochromophoric reconstituted bR within membranes, we will be able to obtain further insight as to whether the observed split CD of the native bR is due to excitonic coupling or coincidental overlap of two or more opposing Cotton effects.

The structural organizations of the PM and apo-membrane are not identical.<sup>52,53</sup> In the case of apo-membrane (**OOO**), it is known that bacterio-opsin (bO) molecules are aligned in a paracrystalline structure.<sup>8,22</sup> Addition of *all-trans*-retinal triggers protein conformational changes leading to steric complementarity and restoration of the hexagonal crystal lattice.<sup>8,23,54,55</sup> Recent experiments using atomic force microscopy have revealed that, although bleaching of the PM results in loss of crystallinity, the trimeric form is preserved.<sup>56-59</sup> This is of primary importance for the following experiments because it is assumed that the trimeric form is maintained throughout, and thus the possibility of excitonic coupling is present in the regenerated pigments.

The regeneration of the pigment, by addition of chromophore to bleached apo-membrane, can be moni-

tored by UV-vis and CD since the spectra reflect the extent of the occupied binding sites.<sup>33</sup> The early stage of regeneration (less than 50%) is characterized by a broad positive CE around the absorption maximum, which turns into a bisignate CD curve, with an increasing negative band becoming apparent after ca. 50% of the binding sites are occupied by the chromophore (although statistical formation of **AOO** and **AAA** is also possible upon addition of 0.33 equiv of retinal, experiments by Ottolenghi and co-workers suggest that filling of apo-membrane takes place sequentially).<sup>44</sup> The CD spectrum of the fully regenerated PM (Fig. 3a), clearly indicates the presence of a bisignate CD peak with a crossover point at 560 nm, in good agreement with the corresponding UV-vis absorption maximum (557 nm). Because the trimeric organization is maintained for the bleached apo-membrane,<sup>56</sup> one could argue that the observed CD spectrum is the result of exciton coupling between the *all-trans*-retinal molecules within the bR trimer.

In order to test the latter hypothesis bleached apo-membrane was reconstituted in a stepwise fashion in the presence of different chromophores to afford heterochromophoric membrane samples. The chromophores used (Fig. 2b) were retinal derivatives with absorption maxima within a 100-nm range. Assuming that in the presence of the retinal analogues, the heterochromophoric PM maintains a similar trimeric organization, one would expect that these chromophores can interact with each other in space, giving rise to a heterochromophoric ECCD spectrum.

Heterochromophoric PM samples were constructed using limited stepwise regeneration of apo-membrane with native *all-trans*-retinal, up to 33% (**AOO**) or 66% (**AAO**), followed by appropriate reconstitution with the second chromophore. The first series of experiments described involve the use of the native *all-trans*-retinal (**A**), merocyanine dye **B**, and retinal analogues **C** and **D** (Fig. 2b). The CD spectra of the fully regenerated homochromophoric pigments with **AAA** and **BBB** are shown in Figure 3a. As can be seen, they both exhibit a bisignate peak with the crossover very close to the maximum absorbance of the corresponding chromophore, ~557 and 646 nm, respectively. The significant difference in the CD intensity can be attributed to the different structural arrangement of the merocyanine chromophores in the trimeric arrangement and/or to the different dipolar strengths. The resemblance between the two sets of bisignate peaks obtained from **AAA** and **BBB** supports the suggestion that both pigments can assume a similar lattice membrane packing.

Formation of the partially reconstituted heterochromophoric pigment **ABO** (66% occupancy) produced the first indication that questions the validity of ECCD as the source of the bisignate appearance of the CD spectra. In this 1:1:0 heterochromophoric system, the CD spectrum reveals the presence of two positive peaks, 544 and 642 nm, that appear to match the UV-vis peaks of the pigment (547 and 640 nm, respectively) in a straightforward manner (Fig. 3b). According to ECCD rule (iv) mentioned above, the small difference of ca. 2700 cm<sup>-1</sup> between the 547 and 640 nm absorption maxima of **A** and **B** should lead to efficient coupling if in fact the two chromophores

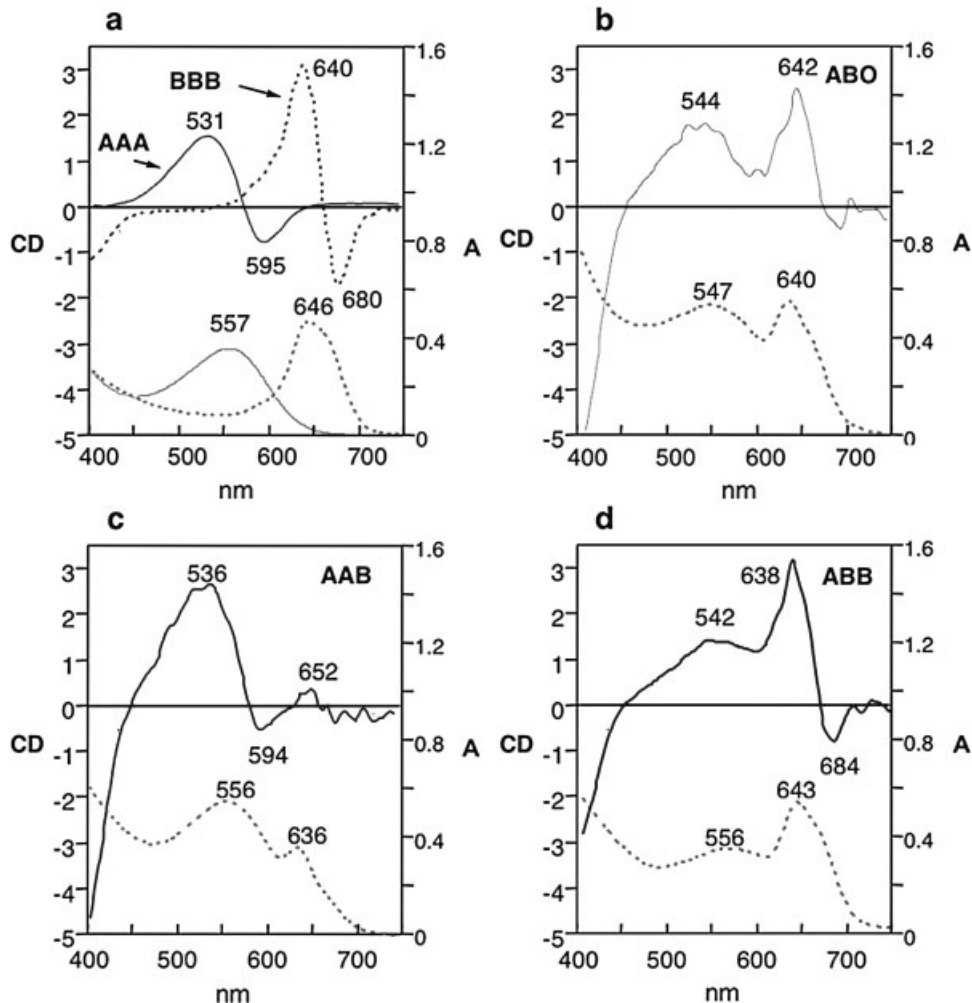


**Fig. 3.** CD (top trace) and UV-vis (bottom trace) of homochromophoric and heterochromophoric bR systems recorded in 20 mM sodium phosphate buffer, pH 7.0: (a) bR (AAA) and mc-bR (BBB); (b) ABO (bR/mc-bR/bO); (c) AAB (bR/mc-bR, 2:1); (d) ABB (bR/mc-bR, 1:2).

are oriented in a manner that allows for exciton coupling. However, the CD appears to represent simple superposition of two Cotton effects associated with two independent chromophores. The small deviations between the UV-vis maxima and the CD crossover wavelength, 557 versus 547 nm for chromophore **A** and 646 versus 640 nm for chromophore **B**, could be ascribed to the difference in binding site environments when all sites are filled as opposed to cases when they are only partly filled. This is also confirmed by the fact that the  $\lambda_{\text{max}}$  of pigment AAA at 557 nm (Fig. 3a) also differs from the  $\lambda_{\text{max}}$  of pigment AOO at 547 nm (Fig. 4a) in which only one-third of the chromophoric binding sites is filled.

For a direct comparison with the fully regenerated system (AAA), heterochromophoric fully reconstituted complexes AAB and ABB were formed. Considering that, as previously discussed, both homochromophoric fully reconstituted complexes AAA and BBB exhibit bisignate CD spectra, one can argue that occupancy of the third binding site is essential for reinstating the correct conformation and structure that leads to the original CD. However, for the heterochromophoric case, even when all the

binding sites are fully occupied (AAB and ABB), there is no evidence of coupling between the two chromophores in either case, as should be present according to ECCD criteria (v) and (vi). Instead, it appears that both UV-vis and CD are simple summations of the component spectra (Fig. 3c,d). Namely, the CD of pigment AAB could be a summation of biphasic **AA** and monophasic **B** spectra while the CD of pigment ABB could be a summation of monophasic **A** and biphasic **BB** spectra. In view of the aforementioned ECCD rules, it is concluded that no exciton-type heterochromophoric interaction is observed between chromophores **A** and **B**. Extrapolation of the latter data to native PM would suggest that the bisignate CD spectrum is not due to EC, although it is possible that fully regenerated homochromophoric systems are required for attaining ECCD. In another words, one could argue that heterochromophoric systems do not achieve the correct conformation for EC, yet the homochromophoric systems are capable of EC due to their unique conformation. The above experiments cannot probe this possibility.

In order to directly address the latter, the CD spectra of bR, partially and fully regenerated, were recorded under

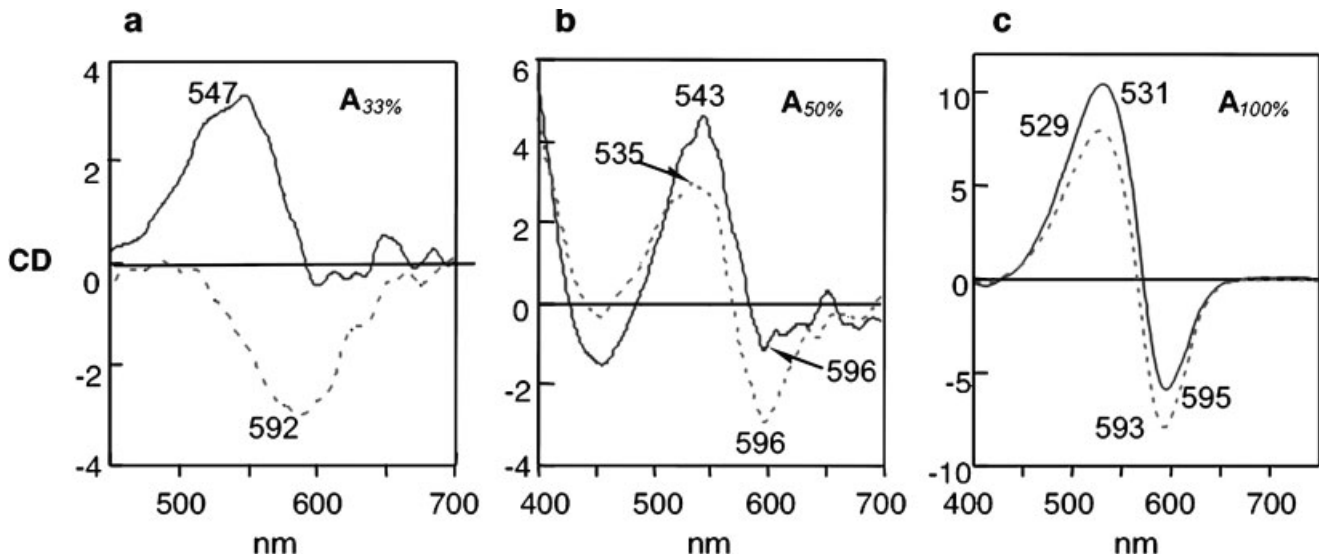


Fig. 4. (a) CD of 33% regenerated PM ( $A_{33\%}$ ) in phosphate buffer (solid line) and the same sample transferred into 50% sucrose in phosphate buffer, pH 7.0 (dashed trace); (b) the same for 50% regenerated and (c) fully regenerated bR.

different conditions to investigate whether or not different environmental factors can influence their shape. Polyhydric alcohols, such as sucrose and glycerol, are known as neutral osmotically active agents and are widely used as protective additives in protein solutions.<sup>60–65</sup> Although the exact molecular mechanism of their effect on proteins and protein assemblies is not clear, direct interactions of the protein with the small molecules and indirect effects mediated by the redistribution of water and lipid molecules have both been implicated.<sup>61,62,66–71</sup> For bR, a continuous network of hydrogen-bound water molecules on the extracellular side of the retinylidene chromophore as well as on the cytoplasmic side have been identified<sup>72–74</sup> and confirmed by the crystal structure.<sup>11</sup> The effects of the osmotically active solutes on the PM structure have been previously studied by applying an osmotic pressure that can withdraw the aforementioned water molecules from the protein interior, distort the protein landscape, and therefore, alter the local environment and the chromophore–protein interactions.<sup>66,67</sup>

As shown in Figure 4a, a solution of 33% regenerated pigment ( $A_{33\%}$ , **AOO**) in phosphate buffer,  $\lambda_{\text{max}}$  557 nm, exhibits a monophasic positive CD at 547 nm; however, upon centrifugation and resuspension of the precipitated pellet in 50% sucrose, the CD undergoes a sign inversion exhibiting a single negative CE at 592 nm (under both conditions, the UV–vis is maintained at 561 nm; data not shown). The CD curves in buffer and sucrose can be reversibly interchanged upon repetition of the centrifugation/resuspension sequence, confirming reversible conformational changes upon solute-induced distortion. Thus, the spectral differences observed are believed to be due to the dramatic effect the medium exerts on the environment of the binding site, resulting in conformational changes.

Further addition of *all-trans*-retinal to the  $A_{33\%}$  buffer suspension yielded the  $A_{50\%}$  pigment. As shown in Fig. 4b, the CD of  $A_{50\%}$  in buffer mostly consisted of a positive

peak at 543 nm, with a very small negative peak at 596 nm. However, when the same sample was resuspended in 50% sucrose solution, a bisignate CD resembling an exciton-coupled system was observed. Further addition of retinal affords pigment **AAA**, which maintains a bisignate curve under both buffer and sucrose conditions (Fig. 4c). At this point, the question remains as to why the sucrose effect does not affect the monomers in the fully regenerated pigment (**AAA**) but induces conformational changes in the partially regenerated pigment ( $A_{33\%}$  and  $A_{50\%}$ ), resulting in significantly altered CD spectra. It is plausible, however, that saturation of the subunits (**AAA**) can lead to a more rigid species that exists in the same conformation under both media.

Although the merocyanine aldehyde is structurally similar to retinal, one can argue that the structural differences can cause additional spectral differences. Therefore, 3,4-dehydroretinal (**C**) and 5,6-dihydroretinal (**D**) were chosen for this study as retinal analogues that can yield red- and blue-shifted pigments, respectively. The CD spectra of both bR **AAA** (Fig. 3a) and mc-bR **BBB** (Fig. 5a) in buffer and sucrose are similar except for minor differences in the crossover wavelengths, thus indicating only minor conformational changes between the two solutions. In contrast, the CD of the red-shifted dehydro-pigment **CCC**,  $\lambda_{\text{max}}$  594 nm (Fig. 5b) in buffer is nearly monophasic with a positive CE at 542 nm, while in sucrose the positive CE is accompanied by a weaker negative CE at 628 nm. This trend is more pronounced in the CD of the blue-shifted bR analogue **DDD**,  $\lambda_{\text{max}}$  467 nm (Fig. 5c), which displays a clear difference in the spectra recorded under different conditions.<sup>46,75</sup> Namely, in sodium phosphate buffer it exhibits a single positive CE at 449 nm, whereas in sucrose it exhibits a bisignate CD with a crossover at 475 nm.

When the trimeric subunits are fully occupied with the same chromophore as in **AAA**, **BBB**, and **CCC**, the simi-

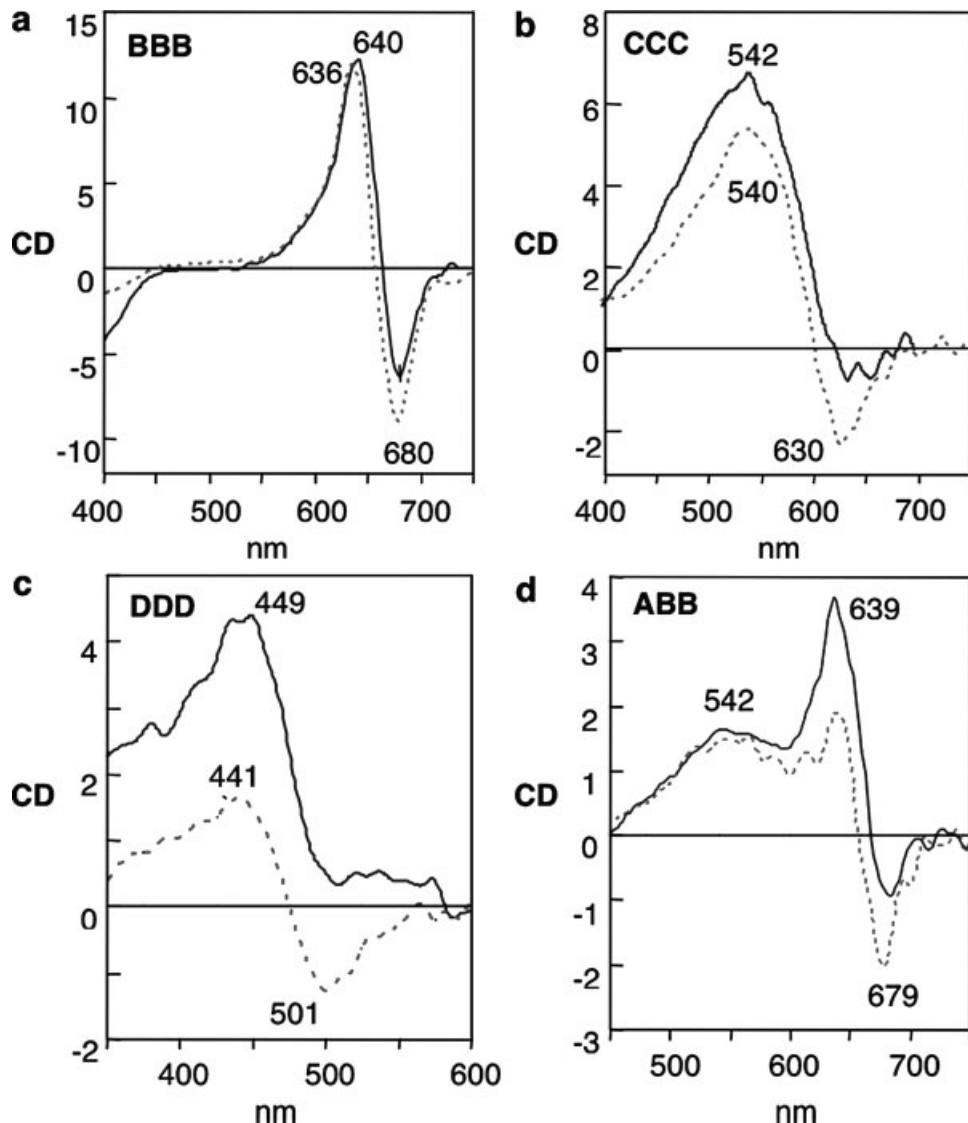


**Fig. 5.** CD of homochromophoric BBB (a), CCC (b), and DDD (c) and heterochromophoric ABB (d) in 20 mM phosphate, pH 7.0 (solid line), and 50% sucrose (dashed line).

larity in the biphasic shape of the CD in phosphate buffer and in 50% sucrose suggest that, in contrast to the partially occupied  $A_{33\%}$  and  $A_{50\%}$  cases, the packed membrane subunits lack conformational flexibility. Similar results were obtained for the heterochromophoric **ABB** system, where the presence of sucrose enhances the negative peak resulting in a more symmetric bisignate shape (Fig. 5d). However, the most dramatic difference was observed for **DDD**, which incorporates the saturated  $\beta$ -ionone ring. While in buffer the CD peak consists of exclusively positive peaks, with a major peak at 449 nm, the 50% sucrose spectrum reveals the presence of a bisignate CD with a negative first CE at 501 nm and a positive CE at 441 nm. The difference in the shape of the two CD spectra can be due to the more flexible nature of the chromophore, which results in different ligand/binding-site interactions. The latter result directly suggests that the apparent bisignate CD in homochromophoric systems is not due to exciton

coupling, and that the bisignate shapes in some of the CD spectra are due to binding site heterogeneity that is medium- and pigment-dependent.

To exclude the possibility of exciton coupling and further investigate the effect of the protein environment on the spectra when the pigment is only partially regenerated, the CD spectra of 33% reconstituted PM ( $A_{33\%}$ ) in four different media (sodium phosphate buffer, 35% and 50% sucrose, and 50% glycerol) were recorded (Fig. 6a). The 33% regenerated PM in phosphate buffer exhibits positive CE, which is consistent with published results.<sup>24</sup> The absence of any negative CE around 590 nm strongly suggests that the amount of randomly formed fully reconstituted PM (**AAA**), if any, is very low and not observed by CD, thus confirming that the distribution of retinal is even amongst the apo-membrane.

Upon examination of the latter data, it is easy to notice that differences in the medium can induce conformational

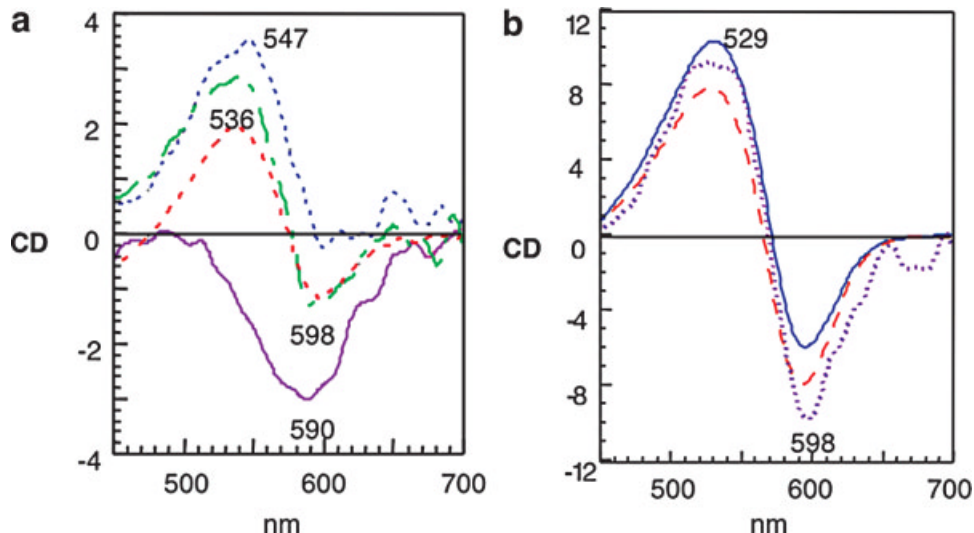


**Fig. 6.** (a) CD of  $A_{33\%}$  in 20 mM phosphate, pH 7.0 buffer (blue), glycerol (green), 35% sucrose (red), and 50% sucrose (magenta). (b) CD of AAA in 20 mM phosphate, pH 7.0 buffer (blue), and in 50% sucrose (red). The purple trace is the physical summation of the four traces of  $A_{33\%}$  presented in (a).

changes leading to different CD spectra. In particular, the spectrum of  $A_{33\%}$  recorded in 35% sucrose is significantly different than that in 50% sucrose. Although the latter consists of a negative peak centered at 592 nm (Fig. 6a), suspension in more dilute sucrose (35%) leads to a bisignate form. In fact, the CD in 35% sucrose of a pigment occupying only 33% of the subunit binding capacity closely matches that of AAA bR. The above result demonstrates that even a single chromophore in the membrane can exhibit a biphasic CD spectrum (Fig. 6a), which is clearly not the result of excitonic interactions between chromophores. Although the possibility exists that a 35% sucrose solution could have forced the disproportionation of  $A_{33\%}$  to yield some fully occupied trimers, this seems very unlikely for large landscapes like PM patches. The spectrum of  $A_{33\%}$  recorded at 50% glycerol also exhibits the biphasic curve, which is significantly different from the one recorded in buffer. This further supports the suggestion that different environmental interactions and/or conformational changes can induce different CD spectra for the same chromophore, even without interaction with other chromophores. These results strengthen arguments proposing that exciton coupling is not the origin of the bisignate curve present in the CD spectrum of native PM. The cumulative spectrum can be due to the superposition of spectra of opposite signs originated from the heterogeneity of the protein environment within the different monomers of the trimeric bR.

Protein–protein, protein–lipid, and protein–chromophore interactions allow numerous possibilities for the chromophores in the trimer to adopt different conformations. The experimental data presented here with partially regenerated PM in various solutes clearly demonstrate the conformational flexibility of the chromophores inside bR. This flexibility is illustrated as a solute-induced chirality (environment-induced conformational changes) observed as CD spectra of opposite signs and/or shapes. The conformational heterogeneity of retinal

chromophores in the bR trimer can be explained as the result of different protein–protein interactions.<sup>52,76</sup> Further evidence for heterogeneity comes from the work of Ottolenghi and Sheves, who demonstrated this through measuring the rate of binding of retinal with the apo-membrane.<sup>44</sup>

In an attempt to further demonstrate that the overall CD of bR could be due to the physical summation of Cotton effects rather than exciton coupling, the three experimental spectra mentioned before,  $A_{33\%}$  in buffer, 50% glycerol, and 50% sucrose were added to yield an apparent CD curve, which closely resembles an actual experimental AAA spectrum (Fig. 6b). The described summation operation, which has no physical meaning demonstrates that an apparent bisignate CD curve, generated by summation of various bR conformations can satisfactorily match the CD of native bR.

Although we believe that the heterochromophoric approach has weakened the arguments for the presence of

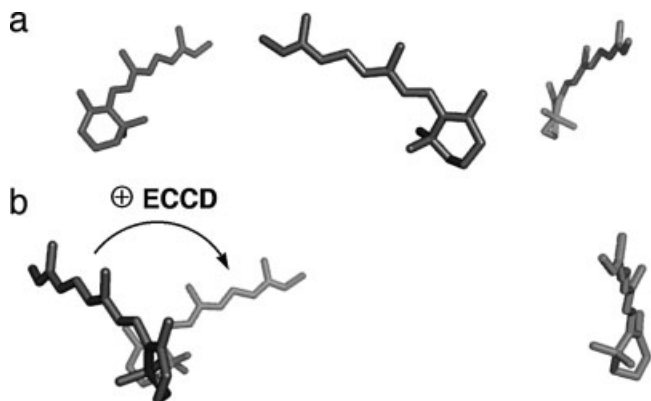


**Fig. 7.** (a) Three all-trans-retinal chromophores as they appear in the crystal structure of PM (trimer) with the protein removed. (b) Chromophores in the PM are arranged in a positive helical orientation.

ECCD in the native PM, one can always contemplate that the homochromophoric systems might enjoy a conformation that is ECCD active, and thus is necessarily different than the heterochromophorically bound membrane. The crystal structure of the trimer could provide another means by which the question can be probed. Figure 1a depicts the three-dimensional structure of the PM. Stripping the protein away, one is left with the disposition of three retinal chromophores (Fig. 7). Inspection of the helicity defined by the chromophores leads to suggestion that if the observed CD spectrum for PM is due to EC, then the expected sign will be positive. In fact, the observed bisignate CD spectrum obtained for PM is negative and thus seems to contradict the expected CD based on the crystal structure of the homochromophoric system. Clearly, it can be argued that neither the crystal structure, nor removing the protein that insulates the chromophores is a true representation of the PM in solution. However, the latter analysis indicates that any anticipated ECCD would have a sign opposite that observed for PM.

In conclusion, the present experimental results using PM preparations with partially or fully occupied subunits, incorporating the same or different chromophores, in different media, along with analysis of the trimer crystal structure support the suggestion that the bisignate curve present in the CD spectrum of bR is not due to interchromophoric EC interactions. Our data directly support the idea of conformational heterogeneity of the chromophores in the bR in the trimer, indicating that the three bR subunits in the trimer are not conformationally equal, thus the bisignate CD spectrum of bR in the purple membrane is a result of the superposition of the CD spectra from variously distorted bR subunits in the trimer rather than interchromophoric exciton-coupled interactions. Although our results appear to agree with recently published observations regarding the suggested heterogeneity of the bR trimer,<sup>44</sup> they do not directly address the issue of when this heterogeneity arises, namely whether the monomers in the unoccupied **OOO** trimer are heterogeneous or the addition of chromophore results in a heterogeneous **AAA** trimer.

### ACKNOWLEDGMENTS

We are grateful for the support received in part through the NIH (GM 36564) to K.N. and the NSF (CAREER, CHE-0094131) to B.B.

### LITERATURE CITED

- Oesterhelt D, Stoeckenius W. Rhodopsin-like protein from purple membrane of *Halobacterium halobium*. *Nat New Biol* 1971;233:149–152.
- Subramaniam S, Hirai T, Henderson R. From structure to mechanism: electron crystallographic studies of bacteriorhodopsin. *Philos Trans R Soc London, Ser A, Math Phys Eng Sci* 2002;360:859–874.
- Khorana HG, Gerber GE, Herlihy WC, Gray CP, Anderegg RJ, Nihei K, Biemann K. Amino-acid sequence of bacteriorhodopsin. *Proc Natl Acad Sci USA* 1979;76:5046–5050.
- Ovchinnikov YA, Abdulaev NG, Feigina MY, Kiselev AV, Lobanov NA. Structural basis of the functioning of bacteriorhodopsin—overview. *FEBS Lett* 1979;100:219–224.
- Bayley H, Huang KS, Radhakrishnan R, Ross AH, Takagaki Y, Khorana HG. Site of attachment of retinal in bacteriorhodopsin. *Proc Natl Acad Sci USA* 1981;78:2225–2229.
- Henderson R, Unwin PNT. 3-Dimensional model of purple membrane obtained by electron microscopy. *Nature* 1975;257:28–32.
- Grigorieff N, Ceska TA, Downing KH, Baldwin JM, Henderson R. Electron-crystallographic refinement of the structure of bacteriorhodopsin. *J Mol Biol* 1996;259:393–421.
- Henderson R. Purple membrane from *Halobacterium halobium*. *Annu Rev Biophys Bioeng* 1977;6:87–109.
- Henderson R, Baldwin JM, Ceska TA, Zemlin F, Beckmann E, Downing KH. An atomic model for the structure of bacteriorhodopsin. *Biochem Soc Trans* 1990;18:844–844.
- Henderson R, Baldwin JM, Ceska TA, Zemlin F, Beckmann E, Downing KH. Model for the structure of bacteriorhodopsin based on high-resolution electron cryomicroscopy. *J Mol Biol* 1990;213:899–929.
- Luecke H, Schobert B, Richter HT, Cartailler JP, Lanyi JK. Structure of bacteriorhodopsin at 1.55 angstrom resolution. *J Mol Biol* 1999;291:899–911.
- Pebay-Peyroula E, Rummel G, Rosenbusch JP, Landau EM. X-ray structure of bacteriorhodopsin at 2.5 angstroms from microcrystals grown in lipidic cubic phases. *Science* 1997;277:1676–1681.
- Essen LO, Siegert R, Lehmann WD, Oesterhelt D. Lipid patches in membrane protein oligomers: crystal structure of the bacteriorhodopsin–lipid complex. *Proc Natl Acad Sci USA* 1998;95:11673–11678.
- Lanyi JK, Luecke H. Bacteriorhodopsin. *Curr Opin Struct Biol* 2001;11:415–419.
- King GI, Mowery PC, Stoeckenius W, Crespi HL, Schoenborn BP. Location of the chromophore in bacteriorhodopsin. *Proc Natl Acad Sci USA* 1980;77:4726–4730.
- Heyn MP. Circular dichroism for determining secondary structure and state of aggregation of membrane proteins. *Methods Enzymol* 1989;172:575–584.
- Gibson NJ, Cassim JY. Evidence for an alpha-II-type helical conformation for bacteriorhodopsin in the purple membrane. *Biochemistry* 1989;28:2134–2139.
- Vogel H, Gartner W. The secondary structure of bacteriorhodopsin determined by Raman and circular-dichroism spectroscopy. *J Biol Chem* 1987;262:11464–11469.
- Heyn MP, Bauer PJ, Dencher NA. Natural CD label to probe structure of purple membrane from *Halobacterium halobium* by means of exciton coupling effects. *Biochem Biophys Res Commun* 1975;67:897–903.
- Heyn MP, Cherry RJ, Müller U. Transient and linear dichroism studies on bacteriorhodopsin—determination of orientation of 568 nm *all-trans*-retinal chromophore. *J Mol Biol* 1977;117:607–620.
- Steinmuller S, Buss V, Gartner W. Circular dichroism spectroscopy of the retinal chromophore during the photocycle of bacteriorhodopsin and its D96N mutant derivative. *J Photochem Photobiol B Biol* 1995;31:139–144.
- Draheim JE, Cassim JY. Effects of polyhydric alcohols on the conformational stability of the purple membrane. *J Membr Biol* 1985;86:229–238.
- Hiraki K, Hamanaka T, Yoshihara K, Kito Y. Bacteriorhodopsin analogs regenerated with enantiomers of 5,6-epoxyretinal. *Biochim Biophys Acta* 1987;891:177–193.
- Wu SG, Elsayed MA. CD spectrum of bacteriorhodopsin—best evidence against exciton model. *Biophys J* 1991;60:190–197.
- Schreckenbach T, Walckhoff B, Oesterhelt D. Specificity of retinal binding-site of bacteriorhodopsin—chemical and stereochemical requirements for binding of retinol and retinal. *Biochemistry* 1978;17:5353–5359.
- Becher B, Ebrey TG. Evidence for chromophore–chromophore (exciton) interaction in purple membrane of *Halobacterium halobium*. *Biochem Biophys Res Commun* 1976;69:1–6.

27. Becher B, Cassim JY. Effects of bleaching and regeneration on purple membrane structure of *Halobacterium halobium*. *Biophys J* 1977;19: 285–297.

28. Muccio DD, Cassim JY. Interpretation of the absorption and circular dichroic spectra of oriented purple membrane films. *Biophys J* 1979; 26:427–440.

29. Muccio DD, Cassim JY. Interpretations of the effects of pH on the spectra of purple membrane. *J Mol Biol* 1979;135:595–609.

30. Cassim JY. Unique biphasic band shape of the visible circular-dichroism of bacteriorhodopsin in purple membrane—excitons, multiple transitions or protein heterogeneity. *Biophys J* 1992;63:1432–1442.

31. Elsayed MA, Karvaly B, Fukumoto JM. Primary step in the bacteriorhodopsin photocycle—photochemistry or excitation transfer. *Proc Natl Acad Sci USA* 1981;78:7512–7516.

32. Elsayed MA, Lin CT, Mason WR. Is there an excitonic interaction or antenna system in bacteriorhodopsin. *Proc Natl Acad Sci USA* 1989; 86:5376–5379.

33. Jang DJ, Elsayed MA, Stern LJ, Mogi T, Khorana HG. Sensitivity of the retinal circular-dichroism of bacteriorhodopsin to the mutagenic single substitution of amino acids—tyrosine. *FEBS Lett* 1990;262: 155–158.

34. Birge RR, Zhang CF. 2-Photon double-resonance spectroscopy of bacteriorhodopsin—assignment of the electronic and dipolar properties of the low-lying 1ag<sup>+</sup>(-)like and 1b-U<sup>+</sup>-like pi,pi<sup>\*</sup> states. *J Chem Phys* 1990;92:7179–7195.

35. Ebrey TG, Becher B, Mao B, Kilbride P, Honig B. Exciton interactions and chromophore orientation in purple membrane. *J Mol Biol* 1977; 112:377–397.

36. London E, Khorana HG. Denaturation and renaturation of bacteriorhodopsin in detergents and lipid–detergent mixtures. *J Biol Chem* 1982;257:7003–7011.

37. Harada NNK. In: Circular dichroic spectroscopy. Mill Valley, CA: University Science Books; 1983. 85–88 p.

38. Nakanishi KB, N. Woody R. Circular dichroism, principles and applications. New York: VHC Publishers, Inc.; 1994.

39. Katre NV, Wolber PK, Stoeckenius W, Stroud RM. Attachment site(s) of retinal in bacteriorhodopsin. *Proc Natl Acad Sci USA* 1981;78: 4068–4072.

40. Derguini F, Caldwell CG, Motto MG, Baloghnaire V, Nakanishi K. Bacteriorhodopsins containing cyanine dye chromophores—support for the external point-charge model. *J Am Chem Soc* 1983;105: 646–648.

41. Henbest H, Jones E, Owen T. Studies in the polyene series. Part LI. Conversion of vitamin A<sub>1</sub> into vitamin A<sub>2</sub>. *J Chem Soc* 1955; 2765–2767.

42. Blatz PE, Dewhurst PB, Balasubramanyan V, Balasubramanyan P, Lin M. Preparation and properties of new visual pigment analogues from 5,6-dihydroretinal and cattle opsin. *Photochem Photobiol* 1970; 11:1–15.

43. Arnaboldi M, Motto MG, Tsujimoto K, Baloghnaire V, Nakanishi K. Hydro-retinals and hydro-rhodopsins. *J Am Chem Soc* 1979;101: 7082–7084.

44. Friedman N, Ottolenghi M, Sheves M. Heterogeneity effects in the binding of *all-trans*-retinal to bacterio-opsin. *Biochemistry* 2003;42: 11281–11288.

45. Tokunaga FE, Ebrey T. The blue membrane: the 3-dehydroretinal based artificial pigment of the purple membrane. *Biochemistry* 1978;17:1915–1922.

46. Nakanishi K, Baloghnaire V, Arnaboldi M, Tsujimoto K, Honig B. An external point-charge model for bacteriorhodopsin to account for its purple color. *J Am Chem Soc* 1980;102:7945–7947.

47. Matile S, Berova N, Nakanishi K. Intramolecular porphyrin pi,pi-stacking: absolute configurational assignment of acyclic compounds with single chiral centers by exciton coupled circular dichroism. *Enantiomer* 1996;1:1–12.

48. Matile S, Berova N, Nakanishi K. Exciton coupled circular dichroic studies of self-assembled brevetoxin–porphyrin conjugates in lipid bilayers and polar solvents. *Chem Biol* 1996;3:379–392.

49. Matile S, Berova N, Nakanishi K, Fleischhauer J, Woody RW. Structural studies by exciton coupled circular dichroism over a large distance: porphyrin derivatives of steroids, dimeric steroids, and brevetoxin B. *J Am Chem Soc* 1996;118:5198–5206.

50. Wiesler WT, Nakanishi K. Relative and absolute configurational assignments of acyclic polyols by circular dichroism. 1. Rationale for a simple procedure based on the exciton chirality method. *J Am Chem Soc* 1989;111:9205–9213.

51. Dong JG, Akratopoulou-Zanze I, Guo JS, Berova N, Nakanishi K, Harada N. Theoretical calculation of circular dichroic exciton-split spectra in presence of three interacting 2-naphthoate chromophores. *Enantiomer* 1997;2:397–409.

52. Booth PJ. Unravelling the folding of bacteriorhodopsin. *Biochim Biophys Acta* 2000;1460:4–14.

53. Dellweg HG, Sumper M. Selective formation of bacterio-opsin trimers by chemical cross-linking of purple membrane. *FEBS Lett* 1978;90: 123–126.

54. Hwang SB, Tseng YW, Stoeckenius W. Spontaneous aggregation of bacteriorhodopsin in brown membrane. *Photochem Photobiol* 1981; 33:419–427.

55. Kollbach G, Steinmuller S, Berndsen T, Buss V, Gartner W. The chromophore induces a correct folding of the polypeptide chain of bacteriorhodopsin. *Biochemistry* 1998;37:8227–8232.

56. Moller C, Buldt G, Dencher NA, Engel A, Muller DJ. Reversible loss of crystallinity on photobleaching purple membrane in the presence of hydroxylamine. *J Mol Biol* 2000;301:869–879.

57. Muller DJ, Heymann JB, Oesterhelt F, Moller C, Gaub H, Buldt G, Engel A. Atomic force microscopy of native purple membrane. *Biochim Biophys Acta* 2000;1460:27–38.

58. Muller DJ, Janovjak H, Lehto T, Kuerschner L, Anderson K. Observing structure, function and assembly of single proteins by AFM. *Prog Biophys Mol Biol* 2002;79:1–43.

59. Stahlberg H, Fotiadis D, Scheuring S, Remigy H, Braun T, Mitsuoka K, Fujiyoshi Y, Engel A. Two-dimensional crystals: a powerful approach to assess structure, function and dynamics of membrane proteins. *FEBS Lett* 2001;504:166–172.

60. Bolen DW, Baskakov IV. The osmophobic effect: natural selection of a thermodynamic force in protein folding. *J Mol Biol* 2001;310:955–963.

61. Chebotareva NA, Andreeva IE, Makeeva VF, Livanova NB, Kurganov BI. Effect of molecular crowding on self-association of phosphorylase kinase and its interaction with phosphorylase b and glycogen. *J Mol Recognit* 2004;17:426–432.

62. Chebotareva NA, Kurganov BI, Livanova NB. Biochemical effects of molecular crowding. *Biochemistry (Moscow)* 2004;69:1239–1251.

63. Lee JC, Timasheff SN. Stabilization of tubulin and other proteins by sucrose. *Fed Proc* 1976;35:1482–1482.

64. Lee JC, Timasheff SN. The stabilization of proteins by sucrose. *J Biol Chem* 1981;256:7193–7201.

65. Price NC. Conformational issues in the characterization of proteins. *Biotechnol Appl Biochem* 2000;31:29–40.

66. Aharoni A, Ottolenghi M, Sheves M. Light-induced hydrolysis and rebinding of nonisomerizable bacteriorhodopsin pigment. *Biophys J* 2002;82:2617–2626.

67. Cao Y, Varo G, Chang M, Ni BF, Needleman R, Lanyi JK. Water is required for proton transfer from aspartate-96 to the bacteriorhodopsin Schiff base. *Biochemistry* 1991;30:10972–10979.

68. Davis-Searles PR, Saunders AJ, Erie DA, Winzor DJ, Pielak GJ. Interpreting the effects of small uncharged solutes on protein-folding equilibria. *Annu Rev Biophys Biomol Struct* 2001;30:271–306.

69. Kim YS, Jones LS, Dong AC, Kendrick BS, Chang BS, Manning MC, Randolph TW, Carpenter JF. Effects of sucrose on conformational equilibria and fluctuations within the native-state ensemble of proteins. *Protein Sci* 2003;12:1252–1261.

70. Mitchell DC, Litman BJ. Effect of protein hydration on receptor conformation: decreased levels of bound water promote metarhodopsin II formation. *Biochemistry* 1999;38:7617–7623.

71. Soderlund T, Alakoskela JMI, Pakkanen AL, Kinnunen PKJ. Comparison of the effects of surface tension and osmotic pressure on the

interfacial hydration of a fluid phospholipid bilayer. *Biophys J* 2003; 85:2333–2341.

72. Edholm O, Berger O, Jahnig F. Structure and fluctuations of bacteriorhodopsin in the purple membrane—a molecular-dynamics study. *J Mol Biol* 1995;250:94–111.

73. Jang H, Crozier PS, Stevens MJ, Woolf TB. How environment supports a state: molecular dynamics simulations of two states in bacteriorhodopsin suggest lipid and water compensation. *Biophys J* 2004;87:129–145.

74. Kandt C, Schlitter J, Gerwert K. Dynamics of water molecules in the bacteriorhodopsin trimer in explicit lipid/water environment. *Biophys J* 2004;86:705–717.

75. Mao B, Govindjee R, Ebrey TG, Arnaboldi M, Baloghnaire V, Nakanishi K, Crouch R. Photochemical and functional-properties of bacteriorhodopsins formed from 5,6-dihydrodesmethylretinals and 5,6-dihydrodesmethylretinals. *Biochemistry* 1981;20:428–435.

76. Hendler RW, Barnett SM, Dracheva S, Bose S, Levin IW. Purple membrane lipid control of bacteriorhodopsin conformational flexibility and photocycle activity—an infrared spectroscopic study. *Eur J Biochem* 2003;270:1920–1925.